

FORMATION OF GLOBULAR CLUSTERS IN GALAXY MERGERS

YUEXING LI, MORDECAI-MARK MAC LOW

Department of Astronomy, Columbia University, New York, NY 10027, USA and
 Department of Astrophysics, American Museum of Natural History, 79th Street at Central Park West, New York, NY 10024-5192, USA

AND

RALF S. KLESSEN

Astrophysikalisches Institut Potsdam, An der Sternwarte 16, D-14482 Potsdam, Germany

Draft version July 17, 2018

ABSTRACT

We present a high-resolution simulation of globular cluster formation in a galaxy merger. For the first time in such a simulation, individual star clusters are directly identified and followed on their orbits. We quantitatively compare star formation in the merger to that in the unperturbed galaxies. The merging galaxies show a strong starburst, in sharp contrast to their isolated progenitors. Most star clusters form in the tidal features. With a mass range of 5×10^5 – $5 \times 10^6 M_{\odot}$, they are identified as globular clusters. The merger remnant is an elliptical galaxy. Clusters with different mass or age have different radial distributions in the galaxy. Our results show that the high specific frequency and bimodal distribution of metallicity observed in elliptical galaxies are natural products of gas-rich mergers, supporting a merger origin for the ellipticals and their globular cluster systems.

Subject headings: galaxies: interactions — galaxies: star clusters — galaxies: starbursts — galaxies: evolution — stars: formation

1. INTRODUCTION

Interactions and mergers drive galactic evolution and cause starbursts. In the past decade, the Hubble Space Telescope (HST) has unveiled evidence for the formation of massive star clusters or young globular clusters in merging galaxies, such as NGC 7252 (Whitmore et al. 1993), the Antennae Galaxy (Whitmore & Schweizer 1995), NGC 3597 (Holtzman et al. 1996), and NGC 3921 (Schweizer et al. 1996), as reviewed by Whitmore (2001).

There have been several theoretical models for the formation of globular clusters (GCs), including primary models where clusters form before galaxies (e.g. Peebles & Dicke 1968), secondary models where clusters form with galaxies (e.g. Fall & Rees 1985; Harris & Pudritz 1994), tertiary models where clusters form after galaxies, such as in mergers (Ashman & Zepf 1992), and unified models (Elmegreen & Efremov 1997). Models have been reviewed by Harris (1991); Ashman & Zepf (1998), and Carney & Harris (2001). The HST observations have prompted particular interest in the merger scenario. There have been many numerical simulations of galaxy mergers (Toomre & Toomre 1972; White 1978; Farouki & Shapiro 1982; Barnes & Hernquist 1992; Hernquist 1992; Mihos & Hernquist 1994, 1996; Dubinski et al. 1999; Springel & White 1999; Springel 2000; Naab & Burkert 2001; Barnes 2002), but only a few focus on GC formation in mergers. These include semi-analytical models (Beasley et al. 2002), combined N-body and smoothed particle hydrodynamics (SPH) simulations (Bekki & Chiba 2002; Bekki et al. 2002), and adaptive-grid cosmological simulations (Kravtsov & Gnedin 2003). In these models individual GCs are not identified and directly followed. In addition, the star formation history of the merger is not compared

to that of the isolated progenitors.

We here model GC formation in both isolated disk galaxies and their mergers using N-body/SPH simulations. Absorbing sink particles are used to directly represent individual massive young star clusters. In § 2 we briefly describe our computational method. We discuss the burst of GC formation during the merging event in § 3, and compare with the evolution of the isolated galaxy. We then focus on the cluster mass and age distribution at the end of the merger in § 4, and summarize in § 5.

2. NUMERICAL METHOD

We use the publicly available SPH code GADGET (Springel et al. 2001), and implement absorbing sink particles that do not interact hydrodynamically (Bate et al. 1995) to directly measure the mass of gravitationally collapsing gas. To represent GCs, we allow sinks to form when the local density exceeds 1000 cm^{-3} (Bromm & Clarke 2002). Our galaxy model consists of a dark matter halo, and a disk of stars and isothermal gas. We follow the analytical work by Mo et al. (1998) and the numerical implementation by Springel & White (1999) and Springel (2000). Our simulations meet three numerical criteria, the Jeans resolution criterion (Bate & Burkert 1997), the gravity-hydro balance criterion for gravitational softening (Bate & Burkert 1997), and the equipartition criterion for particle masses (Steinmetz & White 1997). We adopt a halo concentration parameter $C = 5$, a spin parameter $\lambda = 0.05$, and Hubble constant $H_0 = 70 \text{ km s}^{-1} \text{ Mpc}^{-1}$ (Springel 2000).

The galaxy model studied here initially has rotational velocity $V_{200} = 100 \text{ km s}^{-1}$ at the virial radius where the overdensity is 200, and a virial mass of $M_{200} = 3.3 \times 10^{11} M_{\odot}$. Total mass in the disk and in the disk gas as fraction of the virial mass are $f_d = 0.05$ and $f_g = 0.01$, respectively. An isothermal equation of state with sound

speed $c_s = 6 \text{ km s}^{-1}$ is used. The total particle number for each single galaxy is $N_{\text{tot}} = 1 \times 10^6$, with $N_g = 5 \times 10^5$, $N_d = 2 \times 10^5$, and $N_h = 3 \times 10^5$ for disk gas and stars, and halo dark matter, respectively. The corresponding gravitational softening lengths are $\epsilon_g = 0.01 \text{ kpc}$, $\epsilon_d = 0.1 \text{ kpc}$, and $\epsilon_h = 0.4 \text{ kpc}$. The spatial resolution of the gas is thus 10 pc, and the mass per gas particle is $6.6 \times 10^3 M_\odot$. This is two orders of magnitude better resolution than the models of Bekki et al. (2002).

We perform two simulations. One follows the evolution of the isolated galaxy described above, and the other is an equal-mass, head-on merger of two such galaxies. The two galaxies are on a parabolic orbit and are separated initially by a distance of 300 kpc. In the merger run, $N_{\text{tot}} = 2 \times 10^6$, with $N_g = 1 \times 10^6$ gas particles and corresponding other particle numbers. The simulations are followed for up to 5 Gyr.

3. STARBURSTS IN THE MERGING EVENT

3.1. Where Do Globular Clusters Form?

Our single galaxies begin marginally stable to gravitational instability (Rafikov 2001), with initial Toomre instability parameter for gas $Q = 1.4$. Stars form slowly but steadily, mostly in the center. In the merger event, the galaxies first collide at $t \sim 1.4$ Gyr, then separate to ~ 200 kpc at $t \sim 2$ Gyr, fall back, and finally merge at $t \sim 4.5$ Gyr. Vigorous starbursts occur in each of the two close encounters.

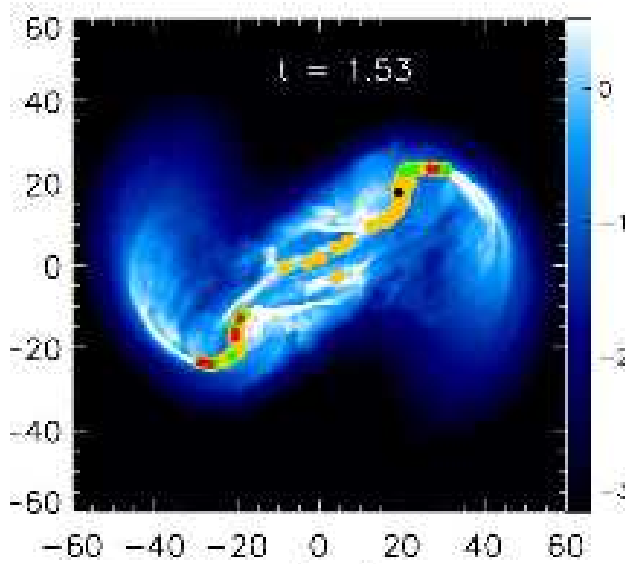


FIG. 1.— GC's formed in the merger. The blue-white image is the gas surface density at $t = 1.53$ Gyr, with values given by the color bar. The colored dots represent (yellow) older GCs with lifetimes $\tau_{\text{gc}} > 10$ Myr, (green) young GCs with $\tau_{\text{gc}} < 10$ Myr and $M_{\text{gc}} < 10^6 M_\odot$, (red) young GCs with $M_{\text{gc}} \geq 10^6 M_\odot$, and (black) the most massive young GC.

Most clusters form during the first close encounter at $t = 1.4\text{--}1.7$ Gyr. To estimate their stellar masses, we make the assumption that individual sink particles represent regions of dense molecular gas. Observations by Rownd & Young (1999) and Wong & Blitz (2002) suggest that the *local* star formation efficiency in molecular

clouds remains roughly constant. We assume that 35% of the mass of each sink particle forms stars, and will show in future work that a range of 20–50% is consistent with the observed Schmidt law. Using this assumption, the cluster mass range is $5 \times 10^5 M_\odot$ to $5 \times 10^6 M_\odot$. We therefore identify these clusters as newly formed GCs.

Figure 1 shows that during the first encounter GCs form in the extended tidal features where the gas reaches high density, in agreement with observations (Whitmore & Schweizer 1995; Zhang et al. 2001). The derived mass range agrees well with spectroscopic estimates by Mengel et al. (2002) of some young clusters in the Antennae Galaxy.

3.2. Comparison Between Merger and Isolated Galaxy

Figure 2 compares star formation in the isolated galaxy with the galaxy merger. In the isolated galaxy, stars start to form at $t \sim 0.3$ Gyr when gravitational instability increases the gas density. The cluster number N_{gc} and mass M_{gc} slowly increase as the galaxy maintains marginal stability. During the merging event, the gas density is locally increased by shocks and tidal forces, leading to starburst behavior. The cluster formation rate dM_{gc}/dt increases dramatically, particularly in the first encounter when more gas is available. At the end of the simulation, $N_{\text{gc}} = 73$ for the isolated galaxy and 417 for the merger.

The specific frequency (Harris & van den Berg 1981) of GCs in a galaxy is $S_{\text{N}} = N_t 10^{0.4(\mathcal{M}_v + 15)}$, where N_t is the total number of GCs, and the V-band absolute magnitude of the host galaxy, $\mathcal{M}_v = \mathcal{M}_\odot - 2.5 \log(L_v/L_\odot)$. We use the method of Bekki et al. (2002) to estimate S_{N} in our models by assuming $M_*/L_v \sim 3$, as in the Milky Way. In order to account for the cluster destruction mechanisms described by Spitzer (1987); Gnedin & Ostriker (1997), and Fall & Zhang (2001), we assume a 10% survival rate of our clusters. Our final derived value of S_{N} depends linearly on this. Each single galaxy has a stellar mass of $M_* \sim 1.65 \times 10^9 M_\odot$, so we can derive $\mathcal{M}_v \sim -17.1$ mag, so $S_{\text{N}} \sim 1.0$. Similarly, the elliptical merger remnant has $M_* \sim 3.3 \times 10^9 M_\odot$, which gives $\mathcal{M}_v \sim -17.9$ mag, and $S_{\text{N}} \sim 3.0$. These values are consistent with observations. For example, the Milky Way-like spiral M31 has $S_{\text{N}} \sim 1.2 \pm 0.2$ (Barmby & Huchra 2001), while typical ellipticals have $S_{\text{N}} \sim 3.5$ (Harris 1991; McLaughlin 1999). These estimates do depend on the stellar mass-to-light ratio of the galaxies (e.g. Larsen et al. 2002; Rhode & Zepf 2004) and survival rate of the clusters (Spitzer 1987; Gnedin & Ostriker 1997; Fall & Zhang 2001; Whitmore 2004). Nevertheless, they reflect the difference between isolated disk galaxies and mergers, and suggest that mergers can explain the considerably higher specific frequency of GCs observed in elliptical galaxies.

4. MERGER REMNANT

Star formation during the merger leads to rapid gas depletion. By $t = 5$ Gyr the two merging galaxies have transformed into an elliptical galaxy, whose stellar distribution is shown in Figure 3. Three distinct populations of GCs form at different epochs, those formed during the two close encounters are almost coeval, as they form over a very short period during the encounters.

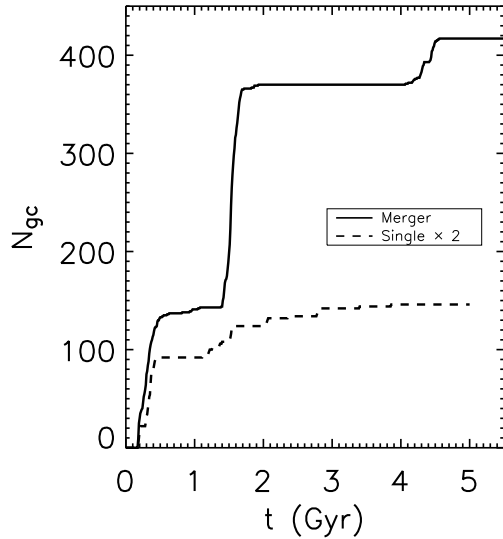


FIG. 2.— Number N_{gc} (top) and fractional mass $M_{\text{gc}}/M_{\text{gas}}$ (bottom) of GCs over time compared between two merging galaxies (solid lines) and the same two galaxies isolated (dashed lines). Note the sudden jumps in the merging galaxies, representing starbursts.

Figure 3 shows the GC system is centered on the stellar spheroid. Massive GCs are concentrated towards the center of the elliptical galaxy that remains after the merger, while less massive ones are found at greater radii as well. Old GCs formed prior to the first encounter and the youngest GCs formed in the second encounter are concentrated towards the center of the galaxy, while GCs formed in the first encounter are also found at large radii. The oldest GCs in our simulation are also the most massive, and quickly sink towards the center by dynamical friction. The youngest ones occur in the galactic center because remaining gas assembles there during the final merger. During the first encounter, on the other hand, GCs form in the tidal tails with greater angular momen-

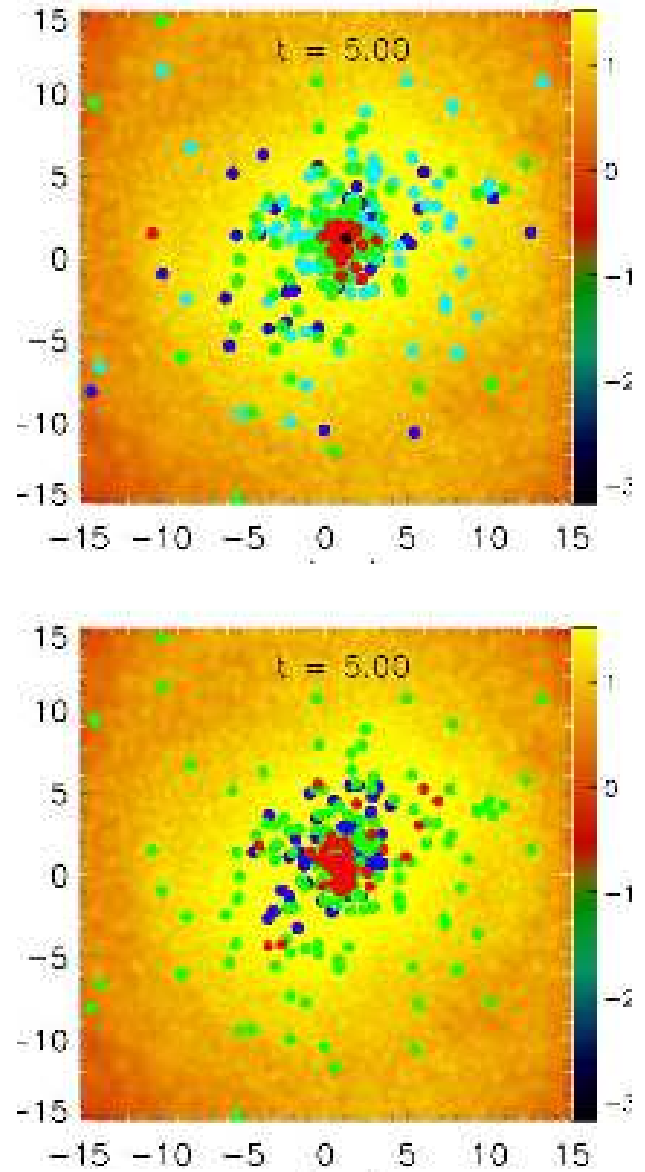


FIG. 3.— Log of stellar surface density in the merger remnant, with values shown in color bar, compared to distribution of GCs (dots) in mass (top panel) and age (bottom panel). Mass bins shown are $M_{\text{gc}} < 10^6 M_{\odot}$ (blue), $10^6 \leq M_{\text{gc}} < 10^{6.5} M_{\odot}$ (cyan), $10^{6.5} \leq M_{\text{gc}} < 10^7 M_{\odot}$ (green), $M_{\text{gc}} \geq 10^7 M_{\odot}$ (red), and the most massive GC, $M_{\text{gc}} = 7.8 \times 10^7 M_{\odot}$ (black). Age bins shown are GCs formed at $t < 1.4$ Gyr during initial approach before the merging event begins (blue), GCs formed at $1.4 \text{ Gyr} < t < 1.9$ Gyr during the first encounter (green), and GCs formed at $4.0 \text{ Gyr} < t < 4.6$ Gyr during the second encounter (red).

tum, and so have a broad radial distribution.

If we assume a metallicity-age relation such that older GCs have lower metallicities (Rich et al. 2001), we clearly see a bimodal metallicity distribution. Young, high-metallicity GCs are centrally concentrated, while older, lower-metallicity GCs extend to larger radii, in agreement with observations (Djorgovski & Meylan 1994). The isolated galaxy forms clusters slowly and steadily, so age, as well as metallicity, follow a smooth

distribution. There is no bimodality. Our results thus support the arguments of Ashman & Zepf (1992) and Kundu & Whitmore (2001) that mergers are required to produce a bimodal distribution.

5. SUMMARY

We present high-resolution simulations of star cluster formation in both a single galaxy and a major merger, using a three-dimensional SPH code that includes absorbing sink particles to represent massive star clusters. This allows direct identification of individual clusters and tracking of their orbital evolution over several gigayears. The merging galaxies show bursts of massive star cluster formation, in sharp contrast to the steady but slow formation in an isolated galaxy. Most new clusters form in the tidal tails and bridges between the merging galaxies. They are identified as progenitors of globular clusters, although it should be emphasized that we do not include dynamical destruction of clusters (e.g. Spitzer 1987; Gnedin & Ostriker 1997; Fall & Zhang 2001) in the simulations. Dynamical destruction will change the number and mass of GCs, affecting our derived specific frequency (where we accounted for it very crudely) and spatial distribution. Inclusion of a destruction model to determine the evolution of our cluster particles will be necessary to fully address these questions.

The estimated specific globular cluster frequency S_N in the elliptical galaxy resulting from the merger exceeds by a factor of 3 that in an isolated galaxy with the same parameters as the merging galaxies, most of the enhancement being in metal-rich GCs. This supports the idea

that the higher S_N of metal-rich GCs observed in ellipticals is produced by mergers. However, elliptical galaxies also show higher S_N for metal-poor GCs. Early mergers could explain this, though other mechanisms have also been proposed (Rhode & Zepf 2004). Clusters formed during different phases of the merger have distinct radial distributions. The spatial distribution of metal-poor old clusters formed before the first encounter as well as of metal-rich younger clusters from the final encounter is centrally concentrated, while clusters formed in the first encounter are more widely dispersed. This suggests the observed multimodal metallicity distribution of globular clusters in elliptical galaxies is the direct result of merger processes.

We thank V. Springel for use of both GADGET and his galaxy initial condition generator, as well as for useful discussions. We also thank A.-K. Jappsen for participating in the implementation of sink particles in GADGET, and K. Bekki, O. Gnedin, R. McCray, M. Shara, and S. Zepf for stimulating discussions, and the anonymous referee for valuable comments that have helped to improve this manuscript. This work was supported by NSF grants AST99-85392 and AST03-07854, NASA grant NAG5-13028, and DFG grant KL1358/1. Computations were performed at the Pittsburgh Supercomputer Center supported by the NSF, on the Parallel Computing Facility of the AMNH, and on an Ultrasparc III cluster generously donated by Sun Microsystems.

REFERENCES

Ashman, K. M., & Zepf, S. E. 1992 *ApJ* 384, 50
 Ashman, K. M., & Zepf, S. E. 1998 *Globular Cluster Systems* (Cambridge University Press)
 Barmby, P. & Huchra, J. P. 2001 *AJ* 122, 2458
 Barnes, J.E. 2002 *MNRAS* 333,481
 Barnes, J.E., & Hernquist, L. 1992 *ARA&A* 30, 705
 Bate, M., Bonnell, I., & Price, N. 1995 *MNRAS* 277, 362
 Bate, M. R. & Burkert, A. 1997 *MNRAS* 288, 1997
 Beasley, M. A. et al. 2002 *MNRAS* 333, 383
 Bekki, K. & Chiba, M. 2002 *MNRAS* 335, 1176
 Bekki, K. et al. 2002 *MNRAS* 335, 1176
 Bromm, V. & Clarke, C. 2002 *ApJ* 566, 1
 Carney, B. W., & Harris, W. E. 2001 *Star Clusters* (Springer)
 Djorgovski, S. & Meylan, G. 1994 *ApJ* 108, 1292
 Dubinski, J., Mihos, C.J., & Hernquist, L. 1999 *ApJ* 526, 607
 Elmegreen, B. G., & Efremov, Y. N. 1997 *ApJ* 480, 235
 Fall, S. M., & Rees, M. J. 1985 *ApJ* 298, 18
 Fall, S. M., & Zhang, Q. 2001 *ApJ* 561, 751
 Farouki, R., & Shapiro, S.L. 1982 *ApJ* 259, 103
 Gnedin, O. Y. & Ostriker, J. P. 1997 *ApJ* 474, 223
 Harris, W. E., 1991 *ARA&A* 29, 543
 Harris, W. E. & Pudritz, R. E. 1994 *ApJ* 429, 177
 Harris, W. E. & van den Berg, S., 1981 *AJ* 86, 1627
 Hernquist, L. 1992 *ApJ* 400, 460
 Holtzman, J.A. et al. 1996 *AJ* 112, 416
 Klessen, R. S., & Burkert, A., 2000 *ApJS*, 128, 287
 Kravtsov, A. V. & Gnedin, O. Y. 2003 *astro-ph/0305199*
 Kundu, A. & Whitmore, B. C. 2001 *AJ* 121, 2950
 Larsen, S. S. et al. 2002 *AJ* 124, 2615
 McLaughlin, D. E. 1999 *AJ*, 117, 2398
 Mengel, S. et al. 2002 *A&A* 383, 137
 Mihos, C.J. & Hernquist, L. 1994 *ApJ* 427, 112
 Mihos, C.J. & Hernquist, L. 1996 *ApJ* 464, 641
 Mo, H. J., Mao, S., & White, S. D. M. 1998 *MNRAS* 295, 319
 Naab, T. & Burkert, A. 2001 *ApJ* 555, 91
 Peebles, P. J. E., & Dicke, R. H. 1968 *ApJ* 154, 891
 Rafikov, R. R. 2001 *MNRAS* 323, 2001
 Rich, R. M., Shara, M. M. & Zurek, D. 2001 *AJ* 122, 842
 Rhode, K. L. & Zepf, S. E. 2004 *AJ* 127, 302
 Rownd, B. K., & Young, J. S. 1999 *AJ* 118, 670
 Schweizer, F. et al. 1996 *AJ* 112, 1839
 Spitzer, L., Jr. 1987 *Dynamical Evolution of Globular Clusters* (Princeton: Princeton Univ. Press)
 Springel, V. 2000 *MNRAS* 312, 859
 Springel, V. & White, S. M. D. 1999 *MNRAS* 307, 162
 Springel, V., Yoshida, N. & White, S. D. M. *New Astron.* 6, 79
 Steinmetz, M. & White, S. D. M. 1997 *MNRAS* 288, 545
 Toomre, A., & Toomre J. 1972 *ApJ* 178, 623
 White, S.D.M. 1978 *MNRAS* 184, 185
 Whitmore, B. et al. 1993 *AJ* 106, 1354
 Whitmore, B. & Schweizer, F. 1995 *AJ* 109, 960
 Whitmore, B. et al. 1999 *AJ* 118, 1551
 Whitmore, B. *astro-ph/0012546*
 Whitmore, B. *astro-ph/0403709*
 Wong, T. & Blitz, L. 2002 *ApJ* 569, 157
 Zhang, Q. & Fall, S. M. 1999 *ApJ* 527, 81
 Zhang, Q., Fall, S. M. & Whitmore, B. 2001 *ApJ* 561, 727

